

RETHINKING PARAMETER SHARING FOR LLM FINE-TUNING WITH MULTIPLE LORAS

000
001
002
003
004
005 **Anonymous authors**
006 Paper under double-blind review
007
008
009
010

ABSTRACT

011 Large language models are often adapted using parameter-efficient techniques
012 such as Low-Rank Adaptation (LoRA), formulated as $y = W_0x + BAx$, where
013 W_0 is the pre-trained parameters and x is the input to the adapted layer. While
014 multi-adapter extensions often employ multiple LoRAs, prior studies suggest that
015 the inner A matrices are highly similar during training and thus suitable for shar-
016 ing. We revisit this phenomenon and find that this similarity is largely attributable
017 to the identical initialization rather than shared knowledge, with B playing a more
018 critical role in knowledge encoding and transfer. Motivated by these insights, we
019 propose **ALoRA**, an asymmetric multi-LoRA design with multiple A matrices
020 and a single shared B in multi-task fine-tuning, and **Fed-ALoRA**, which shares B
021 across clients in federated fine-tuning under both homogeneous and heterogeneous
022 settings, through a novel matrix decomposition strategy to accommodate hetero-
023 geneous ranks across clients. Experiments on commonsense reasoning, math rea-
024 soning, multi-task NLP dataset, and federated NLP dataset demonstrate that our
025 methods achieve more balanced performance across tasks with comparable or su-
026 perior average accuracy relative to existing multi-LoRA approaches.
027

1 INTRODUCTION

028 Large language models (LLMs) have achieved remarkable performance across diverse domains
029 (Achiam et al., 2023; Comanici et al., 2025; Dubey et al., 2024), but the growing scale makes con-
030 ventional full fine-tuning increasingly expensive. Parameter-efficient fine-tuning (PEFT) addresses
031 this challenge by freezing the pre-trained model and updating only a small subset of parameters,
032 improving efficiency while maintaining performance (Han et al., 2024). Among PEFT methods,
033 Low-Rank Adaptation (LoRA) (Hu et al., 2022) is particularly popular: it decomposes weight up-
034 dates into trainable low-rank matrices A and B , which can be merged into the pre-trained model
035 without extra inference latency.
036

037 Recent studies have shown that a single LoRA has limited capacity when handling diverse data
038 distributions (Yang et al., 2024; Cai et al., 2025). A natural extension is to use multiple LoRAs,
039 where each module can specialize in different data modes such as tasks, domains, and distributed
040 clients (Li et al., 2024; Sun et al., 2025; Wu et al., 2024b; Liao et al., 2025). In multi-task fine-
041 tuning, adapters are required to handle task heterogeneity (Liang et al., 2025), and in federated
042 fine-tuning, they should account for client heterogeneity and personalization (Bian et al., 2025).
043 However, naively employing multiple LoRAs also increases computation and communication costs,
044 which makes this approach less efficient.
045

046 To address this problem, recent methods explore parameter sharing across LoRA modules to im-
047 prove parameter efficiency. HydraLoRA (Tian et al., 2024) observes that A matrices trained on
048 different tasks exhibit very high similarity, and proposes a single shared A with multiple B s for
049 multi-task fine-tuning. FedSA-LoRA (Guo et al., 2025) reports similar findings in federated fine-
050 tuning and transmits only A matrices for server aggregation with reduced communication costs.
051 These studies attribute the high similarity in A matrices to the shared knowledge.
052

053 In this paper, we revisit this similarity phenomenon and find that the similarity of A stems mainly
054 from identical initialization rather than shared knowledge. Our analysis of learning dynamics reveals
055 that A functions largely as a feature projector, while B encodes the domain knowledge. A further
056 exploration shows that sharing B yields more effective knowledge transfer than sharing A in both
057

054 multi-task and federated fine-tuning. These insights motivate an interesting but underexplored question: *might sharing the module B, rather than A, be more effective for parameter and knowledge*
 055 *sharing?* In this paper, we provide a positive answer, with our main contributions as follows.
 056

057

- 058 • We propose **ALoRA**, a new asymmetric multi-LoRA architecture for multi-task fine-
 059 tuning. It employs multiple A matrices and a single shared B matrix, where the A matrices
 060 are dynamically routed by the inputs. This design enables each A to explore distinct feature
 061 subspaces while encouraging knowledge transfer through the shared B .
- 062 • We propose **Fed-ALoRA**, which communicates only B matrices rather than full LoRA pa-
 063 rameters for aggregation on server. It supports both homogeneous and heterogeneous set-
 064 tings with the same and different ranks across clients, whereas existing parameter-sharing
 065 federated fine-tuning methods focus only on the homogeneous case. In the homogeneous
 066 setting, Fed-ALoRA updates all A matrices locally, and transmits and aggregates only B
 067 matrices on server side. In the heterogeneous setting, direct aggregation of B is infeasible
 068 due to their distinct sizes, so we decompose B into (B_1, B_2) with appropriate sizes and
 069 introduce an auxiliary matrix for further dimension adjustment. Compared to full LoRA
 070 aggregation, Fed-ALoRA reduces communicated parameters by up to 50% and 75% in the
 071 homogeneous and heterogeneous settings, respectively, while maintaining performance.
- 072 • We conduct extensive experiments on intra-domain multi-task benchmarks such as com-
 073 monsense reasoning and math reasoning, cross-domain multi-task NLP dataset, and fed-
 074 erated NLP dataset to evaluate the effectiveness of our approaches. Across all datasets,
 075 our methods consistently deliver more balanced performance with comparable or su-
 076 perior accuracy compared to existing methods. In particular, **ALoRA** surpasses the sharing-
 077 A approach **HydraLoRA**, improving average ROUGE-1 by +0.68 with a $\Delta m\%$ (which
 078 quantifies performance balance via mean drop from single-objective baselines) gain of -
 079 1.94. Similarly, **Fed-ALoRA** outperforms the sharing- A approach **FedSA-LoRA**, achiev-
 080 ing gains of +1.26 (homogeneous) and +1.96 (heterogeneous) with $\Delta m\%$ gains of -2.08
 081 and -2.65, respectively. Compared with approaches that aggregate full LoRA pa-
 082 rameters, our method attains comparable performance, smaller $\Delta m\%$, and substantially reduced
 083 communication cost by transmitting much fewer parameters.

083 2 BACKGROUND

084 2.1 LOW-RANK ADAPTATION

085 Pre-trained language models exhibit low intrinsic dimensionality when adapt to downstream tasks
 086 (Aghajanyan et al., 2021). LoRA leverages this property by approximating weight updates through
 087 low-rank decomposition. Particularly, for a pre-trained weight matrix $W_0 \in \mathbb{R}^{d_{\text{out}} \times d_{\text{in}}}$, the weight
 088 updates is defined as $\Delta W = BA$, where $A \in \mathbb{R}^{r \times d_{\text{in}}}$, $B \in \mathbb{R}^{d_{\text{out}} \times r}$, and the rank $r \ll \min(d_{\text{in}}, d_{\text{out}})$.
 089 During training, only A and B matrices are trainable. Hence, given the input $x \in \mathbb{R}^{d_{\text{in}}}$, the forward
 090 pass is expressed as: $y = y_0 + \Delta y = W_0x + BAx$. In practice, A is typically initialized using
 091 Kaiming Uniform (He et al., 2015), and B is initialized as zero to ensure $\Delta W = \mathbf{0}$.
 092

093 2.2 FINE-TUNING WITH MULTIPLE LORAS

094 Multiple LoRA-based methods extend vanilla LoRA with additional modules to improve adaptabil-
 095 ity across heterogeneous domains (Zi et al., 2023; Dettmers et al., 2023). In multi-task fine-tuning,
 096 they often use MoE designs where LoRAs act as dynamically routed experts (Luo et al., 2024;
 097 Huang et al., 2024), while in federated fine-tuning, they aim to balance personalization with shared
 098 knowledge aggregation (Raje et al., 2025; Zhang et al., 2025b). A common idea among these multi-
 099 LoRA approaches is to share the same matrix A , based on the observation that A matrices from
 100 LoRAs trained on different tasks or clients are often highly similar. For example, HydraLoRA (Tian
 101 et al., 2024) employs a single A matrix and multiple B matrices to express the weight updates:
 102 $\Delta W = \sum_{i=1}^n w_i B_i A$, where n is the number of B matrices, w_i is the gating score for each B_i .
 103 The federated multi-LoRA approach FedSA-LoRA (Guo et al., 2025) shares only the A matrices
 104 for server aggregation, after which the server broadcasts the aggregated A to all clients. The model
 105 update of client i is given by:
 106

$$107 \Delta W_i^t = B_i^t \bar{A}^t, \quad \bar{A}^t = \text{Agg}(A_1^{t-1}, \dots, A_n^{t-1}),$$

108 where n is the number of clients, and t is the current communication round, and $\text{Agg}(\cdot)$ denotes an
 109 aggregation algorithm such as simple averaging.
 110

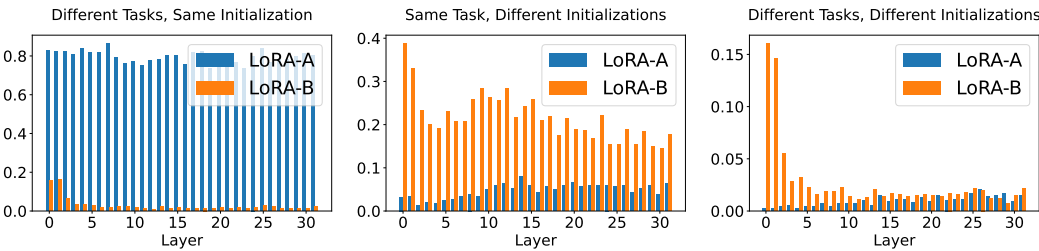
111 3 REVISITING PARAMETER SHARING IN MULTI-LORA FINE-TUNING

113 As noted earlier, a common strategy for parameter sharing is to reuse the same matrix A across
 114 multiple LoRA modules, with the goal of reducing the total number of parameters and enabling
 115 knowledge transfer. In this section, we systematically re-examine this approach through a series of
 116 controlled experiments. Full implementation details are provided in Appendix A.

117 3.1 SIMILARITY IN A STEMS FROM SAME INITIALIZATION, NOT SHARED KNOWLEDGE

119 A primary motivation for sharing A across LoRA modules is the observation that the matrices A_i
 120 of different LoRAs often appear similar during training. However, upon closer examination, we
 121 find that this similarity largely arises from their common initialization rather than from the shared
 122 knowledge. We fine-tune the LLaMA2-7B model (Touvron et al., 2023)¹ separately on classification
 123 and summarization tasks from the Dolly-15K dataset (Conover et al., 2023), using either identical or
 124 different random seeds for A initialization (leading to different initializations for the matrices A_i),
 125 and compare the resulting LoRA modules using principal angle-based similarity (Zhu & Knyazev,
 126 2013), where a value of 1 indicates complete similarity and 0 indicates dissimilarity. The results are
 127 shown in Figure 1, and details of the similarity metric are discussed in Appendix A.1.

128 *Observation.* Figure 1(Left) shows that with the same initialization, A_i matrices are highly similar.
 129 In contrast, Figure 1(Middle, Right) shows that with different initializations, A_i matrices from either
 130 the same or different tasks exhibit little similarity, while B_i matrices display relatively higher simi-
 131 larity. These results suggest that the A is highly sensitive to random seeds rather than necessarily
 132 capturing shared knowledge, whereas B is less affected.



141 Figure 1: Layer-wise similarity analysis between different LoRA modules. Left: two different tasks
 142 with the same random seed. Middle: the same task with different random seeds. Right: two differ-
 143 ent tasks with different random seeds. A_i matrices are similar only under the same initialization,
 144 whereas B_i exhibits relatively stable similarity across different tasks and seeds.

146 3.2 DISSECTING DISTINCT DYNAMICS OF A AND B DURING TRAINING

148 The above analysis motivates us to further investigate the learning dynamics of A and B during
 149 training by comparing their states before and after fine-tuning on the summarization task². Specifi-
 150 cally, we examine the LoRA modules ΔW (see Section 2.2), A and B . Our experiments evaluate (i)
 151 the similarity of modules A and B (using the similarity metric in Section 3.1) and (ii) the magnitude
 152 and directional variations of ΔW , A and B . To formalize this³, any weight matrix $W \in \mathbb{R}^{d_{\text{out}} \times d_{\text{in}}}$
 153 can be decomposed into a magnitude and a direction component: $W = \|W\|_c \frac{W}{\|W\|_c} = mV$, where
 154 $\|\cdot\|_c$ denotes the column-wise norm. Here, $m \in \mathbb{R}^{1 \times d_{\text{in}}}$ is the magnitude vector, with m_j denoting
 155 the norm of the j -th column of W , and $V \in \mathbb{R}^{d_{\text{out}} \times d_{\text{in}}}$ is the direction matrix with unit-norm columns.
 156 Given two matrices W_1 and W_2 , their magnitude and direction discrepancies are defined as

$$157 \Delta M = \frac{1}{d_{\text{in}}} \sum_{j=1}^{d_{\text{in}}} |m_{1,j} - m_{2,j}|, \quad \Delta D = \frac{1}{d_{\text{in}}} \sum_{j=1}^{d_{\text{in}}} (1 - \cos(V_{1,j}, V_{2,j})).$$

160 ¹<https://huggingface.co/meta-llama/Llama-2-7b>

161 ²We use the checkpoints from the second and final steps, since B is initialized to zero at the beginning.

162 ³We follow the same setup as in Liu et al. (2024).

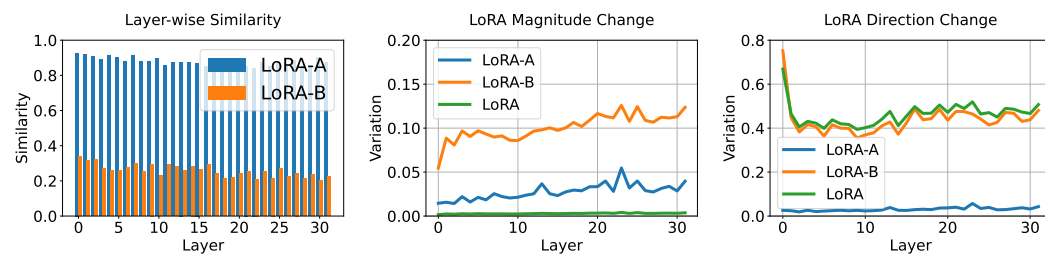


Figure 2: Comparison of LoRA modules before and after the fine-tuning. Left: similarity; Middle: magnitude change; Right: direction change. The module A remains largely unchanged from initialization, whereas the module B exhibits pronounced variation in both magnitude and direction. Overall, LoRA shows limited magnitude change, with nearly all directional change captured by B .

Observation. Figure 2(Left) shows that A remains highly similar throughout training, undergoing only minimal changes, whereas B exhibits much larger differences, indicating substantial adaptation after fine-tuning. Figures 2(Middle, Right) further reveal that the variations in A are primarily in magnitude with little directional change, while B accounts for most of the direction change. These results suggest that A functions more as a fixed feature projector, whereas B aggregates and adapts these features to encode domain knowledge. This highlights the more dominant role of B over A in knowledge learning, raising an intriguing question: might sharing the module B , rather than A , be more effective for parameter and knowledge sharing?

3.3 COMPARISON BETWEEN SHARING A AND SHARING B

In this section, we address the question from Section 3.2 by comparing the performance of sharing modules A and B under both multi-task and federated fine-tuning.

Gradient conflicts may lead to lazy learning for A in multi-task fine-tuning. Given an input $x \in \mathbb{R}^{d_{\text{in}}}$ and the gradient of the output y , $g \in \mathbb{R}^{d_{\text{out}}}$, the gradient of A in the sharing- A structure is $\nabla A = \sum_{i=1}^n w_i (B_i^\top g) x^\top$, where each term corresponds to a B_i expert. We record the magnitudes of ∇A and compute the cosine similarity between gradient components, where negative similarity indicates a conflict that may hinder learning. The same procedure is applied to the sharing- B structure. We then compare the two structures on the common-sense reasoning dataset (Hu et al., 2023), tracking both the gradient magnitudes of shared parameters and the number of conflicts throughout training. The results are shown in Figure 3.

Observation. Figure 3(Left) shows that the gradient magnitude of A in the sharing- A structure is near zero, while the gradient of B in the sharing- B structure is much larger. Figure 3(Right) shows that sharing A also produces more gradient conflicts. Thus, in the sharing- A structure, A learns very slowly possibly due to the more frequent conflicting updates. We refer to this phenomenon as ‘‘lazy learning’’. Previous analysis in Section 3.2 indicates that A functions as a feature projector. Hence, ‘‘lazy learning’’ may restrict the ability to explore diverse feature subspaces.

Knowledge transfer in federated fine-tuning. Each client fine-tunes its own LoRA and transmits the shared parameters to the server, which aggregates and returns them (full details can be found in Section 4.2). This setup allows us to assess whether the shared parameters improve knowledge transfer by evaluating each client’s performance across all tasks. We compare the two structures across 8 clients, each assigned an NLP task from the FLAN dataset (Wei et al., 2022), and use ROUGE-1 score (Lin, 2004) to measure performance, where a value of 0 means no overlap between model prediction and ground truth, and 100 indicates perfect word-level overlap.

216 Table 1: Comparing sharing A versus B in federated fine-tuning. Sharing B consistently outper-
 217 forms sharing A in both the homogeneous and heterogeneous settings.

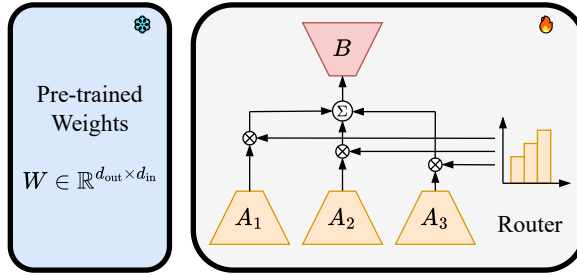
Setting	Method	Client 1	Client 2	Client 3	Client 4	Client 5	Client 6	Client 7	Client 8	Avg.
Homogeneous	Sharing A	50.02	49.78	59.92	42.66	54.05	25.21	23.32	49.43	44.30
	Sharing B	67.43	67.83	69.85	69.26	69.50	60.94	54.86	70.90	66.32
Heterogeneous	Sharing A	43.01	41.58	50.09	38.34	53.53	24.82	24.28	50.41	40.76
	Sharing B	48.38	54.80	58.30	46.98	62.15	35.09	31.80	64.89	50.30

225 *Observation.* As shown in Table 1, in the homogeneous setting, sharing B outperforms sharing A by
 226 an average of 49.71%, with improvements ranging from 16.57% to 141.73%. In the heterogeneous
 227 setting, sharing B achieves an average improvement of 23.41%, with gains ranging from 12.49%
 228 to 41.38%. These results clearly indicate that sharing B better facilitates cross-client knowledge
 229 transfer than sharing A .

230 4 PROPOSED METHODS

232 Motivated by the findings in Section 3, we replace A with B as the shared parameter and propose
 233 two new multi-LoRA fine-tuning methods: **ALoRA** (Asymmetric LoRA) for multi-task training,
 234 and **Fed-ALoRA** for both homogeneous and heterogeneous federated settings.

236 4.1 ALORA FOR MULTI-TASK FINE-TUNING



247 Figure 4: ALoRA adopts multiple A and a single B to explore diverse feature subspaces.

249 Multi-task fine-tuning typically adapts a pre-trained LLM using data from multiple tasks. The goal
 250 is to improve generalization by learning from diverse inputs. The proposed ALoRA is illustrated in
 251 Figure 4. Given an input $x \in \mathbb{R}^{d_{in}}$, the forward pass is given by

$$252 \quad y = y_0 + \Delta y = W_0 x + B \sum_{i=1}^n w_i A_i x,$$

255 where $W_0 \in \mathbb{R}^{d_{out} \times d_{in}}$ is the pre-trained weight matrix, $A_i \in \mathbb{R}^{r \times d_{in}}$ are the expert matrices, $B \in \mathbb{R}^{d_{out} \times r}$ is the shared aggregator, and the rank $r \ll \min(d_{in}, d_{out})$. Each A_i projects the input into a
 256 distinct feature subspace, and B fuses the learned features to produce the output. The expert weights
 257 $w = (w_1, \dots, w_n)$ are obtained from an input-aware router, implemented as a linear gating function
 258 with parameters $W_g \in \mathbb{R}^{n \times d_{in}}$: $w = \text{softmax}(W_g x)$.

260 During the inference, the router computes input-dependent weights, and the weighted average of the
 261 adapters is dynamically merged into the pre-trained weights.

263 4.2 FED-ALORA FOR FEDERATED FINE-TUNING

265 Federated fine-tuning can be divided into two settings: (i) *homogeneous*, where all clients adopt the
 266 same configuration, and (ii) *heterogeneous*, where clients have varying capacities, introducing both
 267 computational and communication heterogeneity.

269 **Homogeneous setting.** In this case, all n clients fine-tune their LoRA modules with the same rank.
 Each update takes the form $\Delta W_i = B_i A_i$, where $A_i \in \mathbb{R}^{r \times d_{in}}$ and $B_i \in \mathbb{R}^{d_{out} \times r}$.

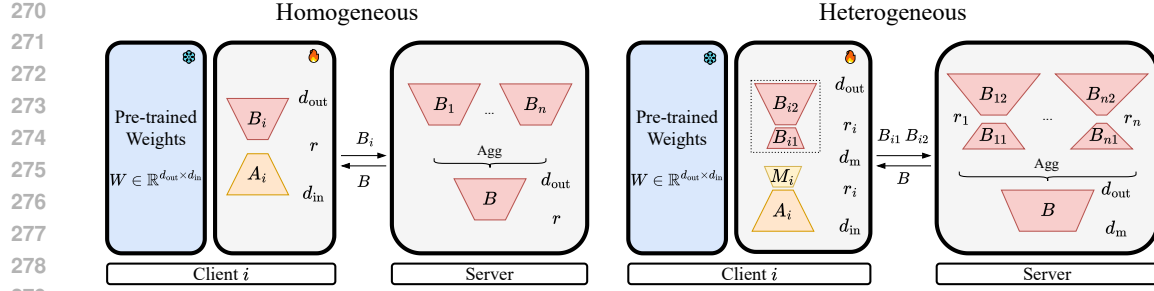


Figure 5: Fed-ALoRA shares only B matrices for server aggregation. Left: Homogeneous setting (same rank), where the shared B is directly transmitted. Right: Heterogeneous setting (different ranks), where the shared B is decomposed into two matrices for heterogeneity. Compared to the standard full LoRA aggregation, the communication cost per client is reduced to $\mathcal{O}(d_{\text{out}}r)$ in the homogeneous setting and $\mathcal{O}(d_{\text{out}}r_i)$ in the heterogeneous setting if d_m is chosen appropriately.

Figure 5(Left) illustrates the procedure of Fed-ALoRA for homogeneous setting, with the detailed steps for each communication round t shown below ($t \geq 1$):

Step 1: **Initialization.** If $t = 1$, each client initializes A_i randomly and sets B_i to zero. For $t > 1$, A_i and B_i are initialized with A_i^{t-1} and B_0^{t-1} , respectively.

Step 2: **Local training.** Each client performs LoRA fine-tuning on its local data, obtaining (A_i^t, B_i^t) by optimizing $\mathcal{L}(W_0 + B_i A_i)$ with respect to (A_i, B_i) , where $\mathcal{L}(\cdot)$ is the loss function. The client then uploads only B_i^t to the server for aggregation.

Step 3: **Aggregation.** The server aggregates the uploaded matrices using the operator $\text{Agg}(\cdot)$ from McMahan et al. (2017), and obtains $B_0^t \leftarrow \text{Agg}(B_1^t, \dots, B_n^t)$.

Step 4: **Broadcast.** The server then sends the global matrix B_0^t back to all clients.

Remark. In the full-LoRA aggregation, each client communicates $(d_{\text{in}} + d_{\text{out}})r$ parameters per round. In contrast, Fed-ALoRA requires transmitting only B_i , reducing the communication cost to $d_{\text{out}}r$.

Heterogeneous setting. In this case, clients may have different capacity constraints, resulting in parameterizations with diverse ranks r_i , given by $\Delta W_i = B_i A_i$, where $A_i \in \mathbb{R}^{r_i \times d_{\text{in}}}$ and $B_i \in \mathbb{R}^{d_{\text{out}} \times r_i}$ for $i = 1, \dots, n$. Because the ranks differ across clients, direct averaging of the B_i matrices is infeasible, and the aggregation strategy used in the homogeneous setting cannot be applied.

To address this issue, we propose a novel decomposition strategy of the form:

$$\Delta W_i = B_{i2} B_{i1} M_i A_i,$$

where $A_i \in \mathbb{R}^{r_i \times d_{\text{in}}}$, $M_i \in \mathbb{R}^{d_m \times r_i}$, $B_{i1} \in \mathbb{R}^{r_i \times d_m}$ and $B_{i2} \in \mathbb{R}^{d_{\text{out}} \times r_i}$. The high-level idea is to decompose the matrix B_i of the same dimension into two components, (B_{i1}, B_{i2}) , each of rank r_i . We further introduce M_i as an intermediate matrix to control the dimension d_m . In addition, every client maintains an accumulator $B_{i0} \in \mathbb{R}^{d_{\text{out}} \times d_m}$ which stores the global updates it has received so far. The full procedure of round t is illustrated in Figure 5(Right) and detailed below:

Step 1: **Initialization.** If $t = 1$, each client initializes (A_i, M_i, B_{i1}) randomly, and sets (B_{i0}, B_{i2}) to zero. For $t > 1$, (A_i, M_i) is initialized with (A_i^{t-1}, M_i^{t-1}) , B_{i0} is initialized with B_0^{t-1} , B_{i1} is re-initialized randomly, and B_{i2} is reset to zero.

Step 2: **Local training.** Each client performs LoRA fine-tuning on its local data, and obtains parameters $(A_i^t, M_i^t, B_{i1}^t, B_{i2}^t)$ by optimizing $\mathcal{L}(W_0 + (B_{i0} + B_{i2} B_{i1}) M_i A_i)$ with respect to $(A_i, M_i, B_{i1}, B_{i2})$. The client then uploads (B_{i1}^t, B_{i2}^t) to the server.

Step 3: **Aggregation.** The server reconstructs $B_i^t = B_{i2}^t B_{i1}^t$ for each client and then performs the aggregation $B_0^t \leftarrow \text{Agg}(B_1^t, \dots, B_n^t)$.

Step 4: **Broadcast.** The server then sends the global matrix B_0^t back to all clients.

Remark. The previous parameter-sharing approach, FedSA-LoRA (Guo et al., 2025), does not support the heterogeneous setting. Fed-ALoRA addresses this limitation by introducing the decomposition (B_{i1}, B_{i2}) , enabling efficient aggregation across clients with different capacities.

324 Table 2: Results on intra-domain multi-task commonsense reasoning benchmark. $\Delta m\%$ measures
 325 performance balance across tasks. \downarrow denotes that lower values are better. All methods use the same
 326 number of adapter parameters. We independently run each experiment 3 times and report the mean
 327 and standard error.

Method	ARC-C	ARC-E	BoolQ	HellaS.	OBQA	PIQA	SIQA	WinoG.	Avg.	$\Delta m\%(\downarrow)$
Single	77.76 \pm 0.97	90.81 \pm 0.23	73.39 \pm 1.05	95.40 \pm 0.08	86.60 \pm 0.72	89.25 \pm 0.47	80.69 \pm 0.48	85.35 \pm 0.64	84.90 \pm 0.21	
LoRA	76.66 \pm 1.02	88.72 \pm 0.83	72.73 \pm 1.24	94.50 \pm 0.41	84.10 \pm 0.14	87.59 \pm 0.15	79.42 \pm 0.15	85.40 \pm 1.00	83.64 \pm 0.27	1.48
LoHa	77.13 \pm 0.13	88.91 \pm 0.09	72.89 \pm 0.19	94.05 \pm 0.23	85.40 \pm 0.56	87.84 \pm 0.34	78.92 \pm 0.44	84.73 \pm 0.17	83.73 \pm 0.11	1.36
AdaLoRA	77.72 \pm 0.72	89.72 \pm 0.96	73.32 \pm 0.19	93.98 \pm 0.73	85.20 \pm 1.13	87.90 \pm 0.35	79.45 \pm 0.18	83.78 \pm 0.28	83.88 \pm 0.32	1.17
MoSLoRA	76.87 \pm 0.12	89.22 \pm 0.15	73.50 \pm 0.86	95.02 \pm 0.13	85.27 \pm 2.58	87.99 \pm 0.59	80.89 \pm 0.12	85.13 \pm 0.55	84.23 \pm 0.39	0.76
HydraLoRA	78.58 \pm 0.12	89.94 \pm 0.18	75.02 \pm 0.18	95.21 \pm 0.11	84.90 \pm 1.55	88.03 \pm 0.15	79.99 \pm 0.72	84.92 \pm 0.34	84.57 \pm 0.17	0.32
ALoRA (ours)	79.40 \pm 0.41	89.69 \pm 0.71	74.38 \pm 0.10	94.85 \pm 0.23	86.10 \pm 0.14	88.24 \pm 0.49	80.17 \pm 0.32	85.68 \pm 0.27	84.81 \pm 0.03	0.04

328
 329
 330
 331
 332
 333
 334
 335 *Remark.* In the vanilla full-LoRA aggregation, each clients uploads $(d_{\text{in}} + d_{\text{out}})r_i$ parameters
 336 to the server. The server then extends all heterogeneous updates to the maximum rank $r_{\text{max}} =$
 337 $\max\{r_1, \dots, r_n\}$ by padding with zeros, and broadcasts $(d_{\text{in}} + d_{\text{out}})r_{\text{max}}$ parameters back to every
 338 client. In Fed-ALoRA, if d_m is chosen comparable to r_{max} with $d_m \ll \min(d_{\text{in}}, d_{\text{out}})$, then client i
 339 maintains $(d_{\text{in}} + d_{\text{out}} + 2d_m)r_i \approx (d_{\text{in}} + d_{\text{out}})r_i$ trainable parameters. The communication cost is
 340 reduced to $\mathcal{O}(d_{\text{out}}r_i)$ from client to server, and $\mathcal{O}(d_{\text{out}}r_{\text{max}})$ from server to clients.

341 5 EXPERIMENTS

342 5.1 MULTI-TASK FINE-TUNING

343 We fine-tune the LLaMA3-8B model (Dubey et al., 2024)⁴ on the *intra-domain* multi-task benchmark
 344 commonsense reasoning (Hu et al., 2023), which contains 8 question answering (QA) datasets,
 345 each focusing on a different aspect of commonsense. We also fine-tune the LLaMA2-7B model
 346 (Touvron et al., 2023)⁵ on the *cross-domain* multi-task NLP dataset (Long et al., 2024), which mixes
 347 8 different tasks such as QA, classification, and text generalization. These tasks are sampled from
 348 the FLAN dataset (Wei et al., 2022). For each task, we first fine-tune LoRA on its own dataset and
 349 use the performance as the single-task baseline. We then compare the proposed ALoRA with several
 350 representative methods: the vanilla LoRA (Hu et al., 2022), LoHa (Yeh et al., 2023), AdaLoRA
 351 (Zhang et al., 2023), MoSLoRA (Wu et al., 2024a), and HydraLoRA (Tian et al., 2024). We also
 352 examine the math reasoning benchmark (Hu et al., 2023). Full details and further discussion are pro-
 353 vided in Appendix B. We also provide additional comparisons between HydraLoRA and ALoRA on
 354 more models in Appendix B.

355 To evaluate performance, we use the following metrics: (1) average accuracy for commonsense
 356 reasoning and average ROUGE-1 score for multi-task NLP dataset; and (2) $\Delta m\%$ (Maninis
 357 et al., 2019), the average per-task performance change against the single-task baseline. $\Delta m\% =$
 358 $\frac{1}{K} \sum_{k=1}^K (-1)^{\delta_k} (M_k - M_0) / M_0 \times 100$, where M_k is the performance of k -th task under the
 359 compared method, M_0 is the baseline performance. $\delta_k = 1$ if higher values indicate better performance,
 360 otherwise $\delta_k = 0$. This metric evaluates how well performance is balanced across multiple tasks.

361 The results are presented in Tables 2 and 3. ALoRA achieves slightly better average accuracy
 362 than existing LoRA variants with the most balanced results in both benchmarks. In commonsense
 363 reasoning, the hardest task is ARC-C, and ALoRA is the only method that exceeds the single-task
 364 baseline. In multi-task NLP dataset, the most challenging task is summarization (Sum), where
 365 ALoRA effectively mitigates negative influence from other tasks and achieves the best performance
 366 on this task. These results suggest that ALoRA encourages knowledge transfer.

367 5.2 FEDERATED FINE-TUNING

368 We fine-tune the LLaMA2-7B model and evaluate on the federated dataset constructed by Long
 369 et al. (2024), which includes 8 NLP tasks sampled from FLAN dataset (Wei et al., 2022), with each
 370 client assigned to one task. For each client, we first fine-tune LoRA on its own training dataset, and
 371 use the performance as the single-client baseline. We use ROUGE-1 as the evaluation metric.

372 In the homogeneous setting, we compare our Fed-ALoRA with: FedIT (Zhang et al., 2024), FedDPA
 373 (Long et al., 2024), and FedSA-LoRA (Guo et al., 2025). In the heterogeneous setting, we compare

374⁴<https://huggingface.co/meta-llama/Meta-Llama-3-8B>

375⁵<https://huggingface.co/meta-llama/Llama-2-7b>

378 Table 3: Results on cross-domain multi-task NLP datasets. $\Delta m\%$ measures performance balance
 379 across tasks. All methods use the same number of adapter parameters.

Method	CSR	Ent	ODQA	Para	RC	Sent	Sum	TFmt	Avg.	$\Delta m\%(\downarrow)$
Single	45.15	65.00	75.19	55.00	78.00	71.75	28.17	88.6	63.36	
LoRA	53.19	63.00	84.31	51.00	50.50	69.50	32.53	89.36	61.67	0.31
LoHa	49.94	60.94	79.78	67.70	69.57	73.50	33.33	90.85	65.70	-5.76
AdaLoRA	51.94	56.94	78.57	65.22	66.61	59.50	31.95	84.93	61.96	-0.41
MoSLoRA	50.70	60.50	81.11	71.50	70.00	75.00	32.64	87.95	66.18	-6.58
HydraLoRA	44.51	67.50	75.83	74.50	76.50	71.50	32.14	89.10	66.45	-6.39
ALoRA (ours)	48.21	62.50	80.35	78.50	68.50	75.00	33.79	90.20	67.13	-8.33

389
 390 Table 4: Results for the **homogeneous** federated setting. Params.(M) denotes the average number
 391 of parameters (in millions) transmitted per client in each round. ALoRA achieves the most balanced
 392 performance while reducing communication cost by 50% compared to full LoRA aggregation FedIT.

Method	Coref	Ent	LAcc	Para	QCls	S2T	TFmt	WSD	Avg.	$\Delta m\%(\downarrow)$	Params.(M)
Single	73.00	84.00	79.00	78.00	94.00	72.21	96.64	60.50	79.67		
FedIT	86.24	86.50	78.00	81.00	94.50	72.06	96.51	65.00	82.47	-3.92	8.39
FedDPA	88.51	85.50	73.50	77.50	95.50	73.76	96.40	65.00	81.96	-3.30	16.78
FedSA-LoRA	81.77	86.00	78.00	75.00	93.50	73.34	96.55	65.00	81.15	-2.21	4.19
Fed-ALoRA (ours)	85.74	87.00	73.50	79.00	94.00	73.10	96.24	71.50	82.51	-4.29	4.19

400 Fed-ALoRA with: ZeroPadding, FLoRA (Wang et al., 2024), and FedSA-LoRA (Guo et al., 2025),
 401 which does not natively support heterogeneity but is adapted here using the decomposition proposed
 402 in our method. We also report the average number of parameters communicated per client in each
 403 round, including both uploads to the server and downloads from the server. In the homogeneous
 404 setting, all clients use rank 8. In the heterogeneous setting, the ranks are $\{64, 64, 32, 32, 16, 16, 8, 8\}$,
 405 with d_m set to 16. Full details are provided in the Appendix B.

406 The results are presented in Table 4 and Table 5. Fed-ALoRA achieves the most balanced performance
 407 while reducing communication cost by 50% compared to full-LoRA aggregation in homogeneous setting,
 408 and reducing by 75% in heterogeneous setting. Notably, the client with the word
 409 sense disambiguation (WSD) task performs poorly. However, Fed-ALoRA outperforms both the
 410 single-client baseline and full-LoRA aggregation in homogeneous setting and ranks second in hetero-
 411 geneous setting. These results show that Fed-ALoRA effectively promotes knowledge sharing
 412 across clients.

413 Table 5: Results for the **heterogeneous** setting. ALoRA achieves the most balanced performance
 414 while reducing communication cost by 75% compared to full LoRA aggregation ZeroPadding. The
 415 original FedSA-LoRA does not support heterogeneity; * denotes implementation with our decom-
 416 position strategy.

Method	Coref	Ent	LAcc	Para	QCls	S2T	TFmt	WSD	Avg.	$\Delta m\%(\downarrow)$	Params.(M)
Single	81.62	88.00	81.00	79.50	94.50	72.07	96.64	60.50	81.73		
ZeroPadding	86.95	87.00	77.50	79.50	94.00	72.87	96.46	64.00	82.29	-0.91	49.28
FLoRA	82.03	87.50	75.50	74.00	95.50	70.99	96.07	62.00	80.45	1.54	141.56
FedSA-LoRA*	80.26	83.50	76.50	76.00	93.00	73.49	96.61	54.00	79.17	3.39	12.12
Fed-ALoRA (ours)	88.27	89.50	79.50	77.00	94.00	72.35	96.37	63.00	82.50	-1.07	12.12

424 5.3 IN-DEPTH ANALYSIS

425 **Multi-task fine-tuning.** We analyze the gate activations of HydraLoRA and ALoRA during inference
 426 on the commonsense reasoning benchmark. Figure 6 presents the t-SNE visualization of the
 427 gate activations in the last layer. The results show that ALoRA activations form clearer clusters
 428 than HydraLoRA. Some tasks share similar gate activations, suggesting that they prefer the same A
 429 experts. This indicates that ALoRA is more effective at capturing diverse feature subspaces across
 430 tasks. In contrast, HydraLoRA relies on a single A matrix, which limits its ability to explore diverse
 431 feature subspaces and leads to more scattered activations.

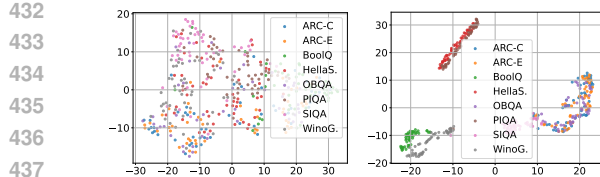


Figure 6: Gate activations of HydraLoRA and ALoRA. ALoRA yields more distinct clusters.

Table 6: Results of different intermediate ranks in the heterogeneous setting.

Fed-ALoRA	Avg.	$\Delta m\%(\downarrow)$
$d_m = 8$	81.92	-0.41
$d_m = 16$	82.50	-1.07
$d_m = 32$	82.25	-0.80
$d_m = 64$	82.37	-1.01

Federated fine-tuning. To further evaluate knowledge sharing, we compare the performance of each client on all tasks between Fed-ALoRA and FedSA-LoRA. This allows us to assess which parameters should be shared to improve cross-client transfer. As shown in Table 1, Fed-ALoRA achieves better results. In addition, we study the effect of different choices of the intermediate rank d_m in the heterogeneous setting. The results in Table 6 show that with a proper choice of d_m , we can reduce the communication cost while maintaining the performance balance.

6 RELATED WORK

Low-rank adaptation. Vanilla LoRA (Hu et al., 2022) reparameterizes weight updates using low-rank matrices, enabling efficient fine-tuning without extra inference latency. Extensions develop along three directions. For rank allocation, AdaLoRA (Zhang et al., 2023) prunes less important singular values, and DyLoRA (Valipour et al., 2023) trains LoRA blocks with different ranks for flexible inference. For memory efficiency, QLoRA (Dettmers et al., 2023) applies 4-bit quantization, and SparseLoRA (Khaki et al., 2025) updates only a sparse subset of parameters using SVD. For structural variation, LoHa and LoKr (Yeh et al., 2023) adopt Hadamard and Kronecker decompositions, and DoRA (Liu et al., 2024) separates magnitude and direction. This paper provides a deep investigation into the training dynamics of modules A and B , demonstrating the more dominant role of B in knowledge learning and transfer.

Multi-task fine-tuning. Fine-tuning on multiple tasks improves generalization and transfer. A popular idea is to integrate LoRA with MoE, where experts specialize in different tasks. Among them, LoRAMoE (Dou et al., 2024), MoELoRA (Luo et al., 2024) and MoRE (Zhang et al., 2025a) align experts with task information to balance performance. SMoRA (Zhao et al., 2025) treats each rank as an expert, and ThanoRA (Liang et al., 2025) builds task-aware LoRA modules. DynMoLE (Li et al., 2025) uses entropy-based routing, and HydraLoRA (Tian et al., 2024) improves parameter efficiency by sharing A matrices. In contrast to HydraLoRA, our proposed **ALoRA** shares matrices B , which promotes diverse feature projections and facilitates more effective knowledge transfer.

Federated fine-tuning. The models are adapted across clients while preserving data privacy. Existing methods fall into homogeneous and heterogeneous settings. In the homogeneous case, FedIT (Zhang et al., 2024) aggregates full LoRA parameters, while FedSA-LoRA (Guo et al., 2025) reduces communication by sharing only A . In the heterogeneous case, HetLoRA (Cho et al., 2024) supports varying ranks via self-pruning with sparse aggregation, Ravan (Raje et al., 2025) introduces multi-head LoRA updates, and FedALT (Bian et al., 2025) employs MoE-based adapters; FLoRA (Wang et al., 2024) provides a unified stacking framework. Unlike FedSA-LoRA, which is restricted to homogeneous ranks, our **Fed-ALoRA** shares B , reducing communication costs while supporting heterogeneous ranks through a decomposition strategy.

7 CONCLUSION

Our study shows that the similarity of LoRAs’ A matrices arises mainly from initialization rather than shared knowledge, with B serving as the key component for knowledge transfer. Building on this insight, we propose ALoRA and Fed-ALoRA, which share B for multi-task and federated fine-tuning. Experiments across diverse benchmarks demonstrate that these methods achieve more balanced performance while maintaining or improving accuracy over existing multi-LoRA approaches. Future work will further examine the distinct learning dynamics of A and B and develop new fine-tuning strategies inspired by these insights.

486 REFERENCES
487

488 Josh Achiam, Steven Adler, Sandhini Agarwal, Lama Ahmad, Ilge Akkaya, Florencia Leoni Ale-
489 man, Diogo Almeida, Janko Altenschmidt, Sam Altman, Shyamal Anadkat, et al. Gpt-4 technical
490 report. *arXiv preprint arXiv:2303.08774*, 2023.

491 Armen Aghajanyan, Sonal Gupta, and Luke Zettlemoyer. Intrinsic dimensionality explains the ef-
492 fectiveness of language model fine-tuning. In *Proceedings of the 59th Annual Meeting of the*
493 *Association for Computational Linguistics and the 11th International Joint Conference on Natu-*
494 *ral Language Processing (Volume 1: Long Papers)*, pp. 7319–7328, 2021.

495

496 Jieming Bian, Lei Wang, Letian Zhang, and Jie Xu. Fedalt: Federated fine-tuning through adaptive
497 local training with rest-of-world lora. *arXiv preprint arXiv:2503.11880*, 2025.

498

499 Yonatan Bisk, Rowan Zellers, Jianfeng Gao, Yejin Choi, et al. Piqa: Reasoning about physical com-
500 monsense in natural language. In *Proceedings of the AAAI Conference on Artificial Intelligence*,
501 volume 34, pp. 7432–7439, 2020.

502

503 Weilin Cai, Juyong Jiang, Fan Wang, Jing Tang, Sunghun Kim, and Jiayi Huang. A survey on
504 mixture of experts in large language models. *IEEE Transactions on Knowledge and Data Engi-*
505 *neering*, 2025.

506

507 Yae Jee Cho, Luyang Liu, Zheng Xu, Aldi Fahrezi, and Gauri Joshi. Heterogeneous lora for fed-
508 erated fine-tuning of on-device foundation models. In *Proceedings of the 2024 Conference on*
509 *Empirical Methods in Natural Language Processing*, pp. 12903–12913, 2024.

510

511 Christopher Clark, Kenton Lee, Ming-Wei Chang, Tom Kwiatkowski, Michael Collins, and Kristina
512 Toutanova. Boolq: Exploring the surprising difficulty of natural yes/no questions. In *Proceedings*
513 *of the 2019 Conference of the North American Chapter of the Association for Computational*
514 *Linguistics: Human Language Technologies, Volume 1 (Long and Short Papers)*, pp. 2924–2936,
515 2019.

516

517 Peter Clark, Isaac Cowhey, Oren Etzioni, Tushar Khot, Ashish Sabharwal, Carissa Schoenick, and
518 Oyvind Tafjord. Think you have solved question answering? try arc, the ai2 reasoning challenge.
519 *arXiv preprint arXiv:1803.05457*, 2018.

520

521 Karl Cobbe, Vineet Kosaraju, Mohammad Bavarian, Mark Chen, Heewoo Jun, Lukasz Kaiser,
522 Matthias Plappert, Jerry Tworek, Jacob Hilton, Reiichiro Nakano, et al. Training verifiers to
523 solve math word problems. *arXiv preprint arXiv:2110.14168*, 2021.

524

525 Gheorghe Comanici, Eric Bieber, Mike Schaeckermann, Ice Pasupat, Noveen Sachdeva, Inderjit
526 Dhillon, Marcel Blistein, Ori Ram, Dan Zhang, Evan Rosen, et al. Gemini 2.5: Pushing the
527 frontier with advanced reasoning, multimodality, long context, and next generation agentic capa-
528 bilities. *arXiv preprint arXiv:2507.06261*, 2025.

529

530 Mike Conover, Matt Hayes, Ankit Mathur, Jianwei Xie, Jun Wan, Sam Shah, Ali Ghodsi, Patrick
531 Wendell, Matei Zaharia, and Reynold Xin. Free dolly: Introducing the world’s first truly open
532 instruction-tuned llm, 2023. URL <https://www.databricks.com/blog/2023/04/12/dolly-first-open-commercially-viable-instruction-tuned-llm>.

533

534 Tim Dettmers, Artidoro Pagnoni, Ari Holtzman, and Luke Zettlemoyer. Qlora: Efficient finetuning
535 of quantized llms. *Advances in Neural Information Processing Systems*, 36:10088–10115, 2023.

536

537 Shihan Dou, Enyu Zhou, Yan Liu, Songyang Gao, Wei Shen, Limao Xiong, Yuhao Zhou, Xiao
538 Wang, Zhiheng Xi, Xiaoran Fan, et al. Loramoe: Alleviating world knowledge forgetting in
539 large language models via moe-style plugin. In *Proceedings of the 62nd Annual Meeting of the*
540 *Association for Computational Linguistics (Volume 1: Long Papers)*, pp. 1932–1945, 2024.

541

542 Abhimanyu Dubey, Abhinav Jauhri, Abhinav Pandey, Abhishek Kadian, Ahmad Al-Dahle, Aiesha
543 Letman, Akhil Mathur, Alan Schelten, Amy Yang, Angela Fan, et al. The llama 3 herd of models.
544 *arXiv e-prints*, pp. arXiv–2407, 2024.

540 Pengxin Guo, Shuang Zeng, Yanran Wang, Huijie Fan, Feifei Wang, and Liangqiong Qu. Selective
 541 aggregation for low-rank adaptation in federated learning. In *The Thirteenth International*
 542 *Conference on Learning Representations*, 2025.

543 Zeyu Han, Chao Gao, Jinyang Liu, Jeff Zhang, and Sai Qian Zhang. Parameter-efficient fine-tuning
 544 for large models: A comprehensive survey. *Transactions on Machine Learning Research*, 2024.
 545 ISSN 2835-8856.

546 Kaiming He, Xiangyu Zhang, Shaoqing Ren, and Jian Sun. Delving deep into rectifiers: Surpassing
 547 human-level performance on imagenet classification. In *Proceedings of the IEEE International*
 548 *Conference on Computer Vision*, pp. 1026–1034, 2015.

549 Edward J Hu, Phillip Wallis, Zeyuan Allen-Zhu, Yuanzhi Li, Shean Wang, Lu Wang, Weizhu Chen,
 550 et al. LoRA: Low-rank adaptation of large language models. In *International Conference on*
 551 *Learning Representations*, 2022.

552 Zhiqiang Hu, Lei Wang, Yihuai Lan, Wanyu Xu, Ee-Peng Lim, Lidong Bing, Xing Xu, Soujanya
 553 Poria, and Roy Lee. Llm-adapters: An adapter family for parameter-efficient fine-tuning of large
 554 language models. In *Proceedings of the 2023 Conference on Empirical Methods in Natural Lan-*
 555 *guage Processing*, pp. 5254–5276, 2023.

556 Chengsong Huang, Qian Liu, Bill Yuchen Lin, Tianyu Pang, Chao Du, and Min Lin. Lorahub: Ef-
 557 ficient cross-task generalization via dynamic lora composition. In *First Conference on Language*
 558 *Modeling*, 2024.

559 Samir Khaki, Xiuyu Li, Junxian Guo, Ligeng Zhu, Konstantinos N Plataniotis, Amir Yazdanbakhsh,
 560 Kurt Keutzer, Song Han, and Zhijian Liu. Sparselora: Accelerating llm fine-tuning with con-
 561 textual sparsity. In *Forty-second International Conference on Machine Learning*, 2025.

562 Rik Koncel-Kedziorski, Subhro Roy, Aida Amini, Nate Kushman, and Hannaneh Hajishirzi.
 563 Mawps: A math word problem repository. In *Proceedings of the 2016 Conference of the North*
 564 *American Chapter of the Association for Computational Linguistics: Human Language Technolo-*
 565 *gies*, pp. 1152–1157, 2016.

566 Dengchun Li, Yingzi Ma, Naizheng Wang, Zhengmao Ye, Zhiyuan Cheng, Yinghao Tang, Yan
 567 Zhang, Lei Duan, Jie Zuo, Cal Yang, et al. Mixlora: Enhancing large language models fine-
 568 tuning with lora-based mixture of experts. *arXiv preprint arXiv:2404.15159*, 2024.

569 Dengchun Li, Naizheng Wang, Zihao Zhang, Haoyang Yin, Lei Duan, Meng Xiao, and Mingjie
 570 Tang. Dynmole: Boosting mixture of lora experts fine-tuning with a hybrid routing mechanism.
 571 *arXiv preprint arXiv:2504.00661*, 2025.

572 Jian Liang, Wenke Huang, Xianda Guo, Guancheng Wan, Bo Du, and Mang Ye. Thanora: Task
 573 heterogeneity-aware multi-task low-rank adaptation. *arXiv preprint arXiv:2505.18640*, 2025.

574 Mengqi Liao, Wei Chen, Junfeng Shen, Shengnan Guo, and Huaiyu Wan. Hmora: Making llms more
 575 effective with hierarchical mixture of lora experts. In *The Thirteenth International Conference on*
 576 *Learning Representations*, 2025.

577 Chin-Yew Lin. Rouge: A package for automatic evaluation of summaries. In *Text Summarization*
 578 *Branches Out*, pp. 74–81, 2004.

579 Wang Ling, Dani Yogatama, Chris Dyer, and Phil Blunsom. Program induction by rationale gener-
 580 ation: Learning to solve and explain algebraic word problems. In *Proceedings of the 55th Annual*
 581 *Meeting of the Association for Computational Linguistics (Volume 1: Long Papers)*, pp. 158–167,
 582 2017.

583 Shih-Yang Liu, Chien-Yi Wang, Hongxu Yin, Pavlo Molchanov, Yu-Chiang Frank Wang, Kwang-
 584 Ting Cheng, and Min-Hung Chen. Dora: Weight-decomposed low-rank adaptation. In *Forty-first*
 585 *International Conference on Machine Learning*, 2024.

586 Guodong Long, Tao Shen, Jing Jiang, Michael Blumenstein, et al. Dual-personalizing adapter for
 587 federated foundation models. *Advances in Neural Information Processing Systems*, 37:39409–
 588 39433, 2024.

594 Tongxu Luo, Jiahe Lei, Fangyu Lei, Weihao Liu, Shizhu He, Jun Zhao, and Kang Liu. Moelora:
 595 Contrastive learning guided mixture of experts on parameter-efficient fine-tuning for large lan-
 596 guage models. *arXiv preprint arXiv:2402.12851*, 2024.

597

598 Kevis-Kokitsi Maninis, Ilija Radosavovic, and Iasonas Kokkinos. Attentive single-tasking of multi-
 599 ple tasks. In *Proceedings of the IEEE/CVF Conference on Computer Vision and Pattern Recog-
 600 nition*, pp. 1851–1860, 2019.

601 Brendan McMahan, Eider Moore, Daniel Ramage, Seth Hampson, and Blaise Aguera y Arcas.
 602 Communication-efficient learning of deep networks from decentralized data. In *Artificial Intelli-
 603 gence and Statistics*, pp. 1273–1282. PMLR, 2017.

604

605 Todor Mihaylov, Peter Clark, Tushar Khot, and Ashish Sabharwal. Can a suit of armor conduct elec-
 606 tricity? a new dataset for open book question answering. In *Proceedings of the 2018 Conference
 607 on Empirical Methods in Natural Language Processing*, pp. 2381–2391, 2018.

608

609 Niklas Muennighoff, Thomas Wang, Lintang Sutawika, Adam Roberts, Stella Biderman, Teven
 610 Le Scao, M Saiful Bari, Sheng Shen, Zheng-Xin Yong, Hailey Schoelkopf, et al. Crosslingual
 611 generalization through multitask finetuning. In *Proceedings of the 61st Annual Meeting of the
 612 Association for Computational Linguistics (Volume 1: Long Papers)*, pp. 15991–16111, 2023.

613

614 Arkil Patel, Satwik Bhattacharya, and Navin Goyal. Are nlp models really able to solve simple
 615 math word problems? In *Proceedings of the 2021 Conference of the North American Chapter of
 616 the Association for Computational Linguistics: Human Language Technologies*, pp. 2080–2094,
 617 2021.

618

619 Arian Raje, Baris Askin, Divyansh Jhunjhunwala, and Gauri Joshi. Ravan: Multi-head low-rank
 620 adaptation for federated fine-tuning. *arXiv preprint arXiv:2506.05568*, 2025.

621

622 Keisuke Sakaguchi, Ronan Le Bras, Chandra Bhagavatula, and Yejin Choi. Winogrande: An adver-
 623 sarial winograd schema challenge at scale. *Communications of the ACM*, 64(9):99–106, 2021.

624

625 Maarten Sap, Hannah Rashkin, Derek Chen, Ronan Le Bras, and Yejin Choi. Social iqa: Common-
 626 sense reasoning about social interactions. In *Proceedings of the 2019 Conference on Empirical
 627 Methods in Natural Language Processing and the 9th International Joint Conference on Natural
 628 Language Processing (EMNLP-IJCNLP)*, pp. 4463–4473, 2019.

629

630 Mengyang Sun, Yihao Wang, Tao Feng, Dan Zhang, Yifan Zhu, and Jie Tang. A stronger mixture
 631 of low-rank experts for fine-tuning foundation models. In *Forty-second International Conference
 632 on Machine Learning*, 2025.

633

634 Rohan Taori, Ishaan Gulrajani, Tianyi Zhang, Yann Dubois, Xuechen Li, Carlos Guestrin, Percy
 635 Liang, and Tatsunori B. Hashimoto. Stanford alpaca: An instruction-following llama model.
 636 https://github.com/tatsu-lab/stanford_alpaca, 2023.

637

638 Chunlin Tian, Zhan Shi, Zhijiang Guo, Li Li, and Cheng-Zhong Xu. Hydralora: An asymmetric
 639 lora architecture for efficient fine-tuning. *Advances in Neural Information Processing Systems*,
 640 37:9565–9584, 2024.

641

642 Hugo Touvron, Louis Martin, Kevin Stone, Peter Albert, Amjad Almahairi, Yasmine Babaei, Niko-
 643 lay Bashlykov, Soumya Batra, Prajjwal Bhargava, Shruti Bhosale, et al. Llama 2: Open founda-
 644 tion and fine-tuned chat models. *arXiv preprint arXiv:2307.09288*, 2023.

645

646 Mojtaba Valipour, Mehdi Rezagholizadeh, Ivan Kobyzev, and Ali Ghodsi. Dylora: Parameter-
 647 efficient tuning of pre-trained models using dynamic search-free low-rank adaptation. In *Pro-
 648 ceedings of the 17th Conference of the European Chapter of the Association for Computational
 649 Linguistics*, pp. 3274–3287, 2023.

650

651 Ziyao Wang, Zheyu Shen, Yexiao He, Guoheng Sun, Hongyi Wang, Lingjuan Lyu, and Ang Li.
 652 Flora: Federated fine-tuning large language models with heterogeneous low-rank adaptations.
 653 *Advances in Neural Information Processing Systems*, 37:22513–22533, 2024.

648 Jason Wei, Maarten Bosma, Vincent Zhao, Kelvin Guu, Adams Wei Yu, Brian Lester, Nan Du, An-
 649 drew M Dai, and Quoc V Le. Finetuned language models are zero-shot learners. In *International*
 650 *Conference on Learning Representations*, 2022.

651

652 Taiqiang Wu, Jiahao Wang, Zhe Zhao, and Ngai Wong. Mixture-of-subspaces in low-rank adapta-
 653 tion. In *Proceedings of the 2024 Conference on Empirical Methods in Natural Language Pro-*
 654 *cessing*, pp. 7880–7899, 2024a.

655 Xun Wu, Shaohan Huang, and Furu Wei. Mixture of lora experts. In *The Twelfth International*
 656 *Conference on Learning Representations*, 2024b.

657

658 An Yang, Anfeng Li, Baosong Yang, Beichen Zhang, Binyuan Hui, Bo Zheng, Bowen Yu,
 659 Chang Gao, Chengan Huang, Chenxu Lv, et al. Qwen3 technical report. *arXiv preprint*
 660 *arXiv:2505.09388*, 2025.

661 Menglin Yang, Jialin Chen, Yifei Zhang, Jiahong Liu, Jiasheng Zhang, Qiyao Ma, Harshit Verma,
 662 Qianru Zhang, Min Zhou, Irwin King, et al. Low-rank adaptation for foundation models: A
 663 comprehensive review. *arXiv preprint arXiv:2501.00365*, 2024.

664 Shih-Ying Yeh, Yu-Guan Hsieh, Zhidong Gao, Bernard BW Yang, Giyeong Oh, and Yanmin Gong.
 665 Navigating text-to-image customization: From lycoris fine-tuning to model evaluation. In *The*
 666 *Twelfth International Conference on Learning Representations*, 2023.

667

668 Rowan Zellers, Ari Holtzman, Yonatan Bisk, Ali Farhadi, and Yejin Choi. Hellaswag: Can a ma-
 669 chine really finish your sentence? In *Proceedings of the 57th Annual Meeting of the Association*
 670 *for Computational Linguistics*, pp. 4791–4800, 2019.

671 Dacao Zhang, Kun Zhang, Shimao Chu, Le Wu, Xin Li, and Si Wei. More: A mixture of low-rank
 672 experts for adaptive multi-task learning. *arXiv preprint arXiv:2505.22694*, 2025a.

673

674 Jianyi Zhang, Saeed Vahidian, Martin Kuo, Chunyuan Li, Ruiyi Zhang, Tong Yu, Guoyin Wang, and
 675 Yiran Chen. Towards building the federatedgpt: Federated instruction tuning. In *ICASSP 2024-*
 676 *2024 IEEE International Conference on Acoustics, Speech and Signal Processing (ICASSP)*, pp.
 677 6915–6919. IEEE, 2024.

678

679 Qingru Zhang, Minshuo Chen, Alexander Bukharin, Pengcheng He, Yu Cheng, Weizhu Chen, and
 680 Tuo Zhao. Adaptive budget allocation for parameter-efficient fine-tuning. In *The Eleventh Inter-*
 681 *national Conference on Learning Representations*, 2023.

682

683 Zikai Zhang, Ping Liu, Jiahao Xu, and Rui Hu. Fed-hello: Efficient federated foundation model
 684 fine-tuning with heterogeneous lora allocation. *arXiv preprint arXiv:2506.12213*, 2025b.

685

686 Ziyu Zhao, Yixiao Zhou, Zhi Zhang, Didi Zhu, Tao Shen, Zexi Li, Jinluan Yang, Xuwu Wang, Jing
 687 Su, Kun Kuang, et al. Each rank could be an expert: Single-ranked mixture of experts lora for
 688 multi-task learning. *arXiv preprint arXiv:2501.15103*, 2025.

689

690 Peizhen Zhu and Andrew V Knyazev. Angles between subspaces and their tangents. *Journal of*
 691 *Numerical Mathematics*, 21(4):325–340, 2013.

692

693 Bojia Zi, Xianbiao Qi, Lingzhi Wang, Jianan Wang, Kam-Fai Wong, and Lei Zhang. Delta-
 694 lora: Fine-tuning high-rank parameters with the delta of low-rank matrices. *arXiv preprint*
 695 *arXiv:2309.02411*, 2023.

696

697

698

699

700

701

702
703
704
705
706
707
SUPPLEMENTARY MATERIALS708
709
710
711
A ADDITIONAL DETAILS FOR SECTION 3712
713
714
715
A.1 SIMILARITY METRIC IN LoRA MODULES716
717
718
719
720
LoRA represents the weight updates as $\Delta W = BA$ with $A \in \mathbb{R}^{r \times d_{\text{in}}}$, $B \in \mathbb{R}^{d_{\text{out}} \times r}$. For any
invertible $R \in \mathbb{R}^{r \times r}$, we have

721
722
$$\Delta W = BA = (BR)(R^{-1}A).$$

723
724
725
726
727
728
729
730
731
This shows that A and B are not individually unique. They can be arbitrarily rotated within the rank-
 r subspace without changing ΔW . As a result, directly computing the cosine similarity between A
or B matrices can give misleading results.732
733
734
735
736
737
738
739
740
741
742
743
744
745
746
747
748
749
750
751
752
753
754
755
756
757
758
759
760
761
762
763
764
765
766
767
768
769
770
771
772
773
774
775
776
777
778
779
780
781
782
783
784
785
786
787
788
789
790
791
792
793
794
795
796
797
798
799
800
801
802
803
804
805
806
807
808
809
810
811
812
813
814
815
816
817
818
819
820
821
822
823
824
825
826
827
828
829
830
831
832
833
834
835
836
837
838
839
840
841
842
843
844
845
846
847
848
849
850
851
852
853
854
855
856
857
858
859
860
861
862
863
864
865
866
867
868
869
870
871
872
873
874
875
876
877
878
879
880
881
882
883
884
885
886
887
888
889
890
891
892
893
894
895
896
897
898
899
900
901
902
903
904
905
906
907
908
909
910
911
912
913
914
915
916
917
918
919
920
921
922
923
924
925
926
927
928
929
930
931
932
933
934
935
936
937
938
939
940
941
942
943
944
945
946
947
948
949
950
951
952
953
954
955
956
957
958
959
960
961
962
963
964
965
966
967
968
969
970
971
972
973
974
975
976
977
978
979
980
981
982
983
984
985
986
987
988
989
990
991
992
993
994
995
996
997
998
999
1000
1001
1002
1003
1004
1005
1006
1007
1008
1009
1010
1011
1012
1013
1014
1015
1016
1017
1018
1019
1020
1021
1022
1023
1024
1025
1026
1027
1028
1029
1030
1031
1032
1033
1034
1035
1036
1037
1038
1039
1040
1041
1042
1043
1044
1045
1046
1047
1048
1049
1050
1051
1052
1053
1054
1055
1056
1057
1058
1059
1060
1061
1062
1063
1064
1065
1066
1067
1068
1069
1070
1071
1072
1073
1074
1075
1076
1077
1078
1079
1080
1081
1082
1083
1084
1085
1086
1087
1088
1089
1090
1091
1092
1093
1094
1095
1096
1097
1098
1099
1100
1101
1102
1103
1104
1105
1106
1107
1108
1109
1110
1111
1112
1113
1114
1115
1116
1117
1118
1119
1120
1121
1122
1123
1124
1125
1126
1127
1128
1129
1130
1131
1132
1133
1134
1135
1136
1137
1138
1139
1140
1141
1142
1143
1144
1145
1146
1147
1148
1149
1150
1151
1152
1153
1154
1155
1156
1157
1158
1159
1160
1161
1162
1163
1164
1165
1166
1167
1168
1169
1170
1171
1172
1173
1174
1175
1176
1177
1178
1179
1180
1181
1182
1183
1184
1185
1186
1187
1188
1189
1190
1191
1192
1193
1194
1195
1196
1197
1198
1199
1200
1201
1202
1203
1204
1205
1206
1207
1208
1209
1210
1211
1212
1213
1214
1215
1216
1217
1218
1219
1220
1221
1222
1223
1224
1225
1226
1227
1228
1229
1230
1231
1232
1233
1234
1235
1236
1237
1238
1239
1240
1241
1242
1243
1244
1245
1246
1247
1248
1249
1250
1251
1252
1253
1254
1255
1256
1257
1258
1259
1260
1261
1262
1263
1264
1265
1266
1267
1268
1269
1270
1271
1272
1273
1274
1275
1276
1277
1278
1279
1280
1281
1282
1283
1284
1285
1286
1287
1288
1289
1290
1291
1292
1293
1294
1295
1296
1297
1298
1299
1300
1301
1302
1303
1304
1305
1306
1307
1308
1309
1310
1311
1312
1313
1314
1315
1316
1317
1318
1319
1320
1321
1322
1323
1324
1325
1326
1327
1328
1329
1330
1331
1332
1333
1334
1335
1336
1337
1338
1339
1340
1341
1342
1343
1344
1345
1346
1347
1348
1349
1350
1351
1352
1353
1354
1355
1356
1357
1358
1359
1360
1361
1362
1363
1364
1365
1366
1367
1368
1369
1370
1371
1372
1373
1374
1375
1376
1377
1378
1379
1380
1381
1382
1383
1384
1385
1386
1387
1388
1389
1390
1391
1392
1393
1394
1395
1396
1397
1398
1399
1400
1401
1402
1403
1404
1405
1406
1407
1408
1409
1410
1411
1412
1413
1414
1415
1416
1417
1418
1419
1420
1421
1422
1423
1424
1425
1426
1427
1428
1429
1430
1431
1432
1433
1434
1435
1436
1437
1438
1439
1440
1441
1442
1443
1444
1445
1446
1447
1448
1449
1450
1451
1452
1453
1454
1455
1456
1457
1458
1459
1460
1461
1462
1463
1464
1465
1466
1467
1468
1469
1470
1471
1472
1473
1474
1475
1476
1477
1478
1479
1480
1481
1482
1483
1484
1485
1486
1487
1488
1489
1490
1491
1492
1493
1494
1495
1496
1497
1498
1499
1500
1501
1502
1503
1504
1505
1506
1507
1508
1509
1510
1511
1512
1513
1514
1515
1516
1517
1518
1519
1520
1521
1522
1523
1524
1525
1526
1527
1528
1529
1530
1531
1532
1533
1534
1535
1536
1537
1538
1539
1540
1541
1542
1543
1544
1545
1546
1547
1548
1549
1550
1551
1552
1553
1554
1555
1556
1557
1558
1559
1560
1561
1562
1563
1564
1565
1566
1567
1568
1569
1570
1571
1572
1573
1574
1575
1576
1577
1578
1579
1580
1581
1582
1583
1584
1585
1586
1587
1588
1589
1590
1591
1592
1593
1594
1595
1596
1597
1598
1599
1600
1601
1602
1603
1604
1605
1606
1607
1608
1609
1610
1611
1612
1613
1614
1615
1616
1617
1618
1619
1620
1621
1622
1623
1624
1625
1626
1627
1628
1629
1630
1631
1632
1633
1634
1635
1636
1637
1638
1639
1640
1641
1642
1643
1644
1645
1646
1647
1648
1649
1650
1651
1652
1653
1654
1655
1656
1657
1658
1659
1660
1661
1662
1663
1664
1665
1666
1667
1668
1669
1670
1671
1672
1673
1674
1675
1676
1677
1678
1679
1680
1681
1682
1683
1684
1685
1686
1687
1688
1689
1690
1691
1692
1693
1694
1695
1696
1697
1698
1699
1700
1701
1702
1703
1704
1705
1706
1707
1708
1709
1710
1711
1712
1713
1714
1715
1716
1717
1718
1719
1720
1721
1722
1723
1724
1725
1726
1727
1728
1729
1730
1731
1732
1733
1734
1735
1736
1737
1738
1739
1740
1741
1742
1743
1744
1745
1746
1747
1748
1749
1750
1751
1752
1753
1754
1755
1756
1757
1758
1759
17510
17511
17512
17513
17514
17515
17516
17517
17518
17519
17520
17521
17522
17523
17524
17525
17526
17527
17528
17529
17530
17531
17532
17533
17534
17535
17536
17537
17538
17539
17540
17541
17542
17543
17544
17545
17546
17547
17548
17549
17550
17551
17552
17553
17554
17555
17556
17557
17558
17559
17560
17561
17562
17563
17564
17565
17566
17567
17568
17569
17570
17571
17572
17573
17574
17575
17576
17577
17578
17579
17580
17581
17582
17583
17584
17585
17586
17587
17588
17589
17590
17591
17592
17593
17594
17595
17596
17597
17598
17599
175100
175101
175102
175103
175104
175105
175106
175107
175108
175109
175110
175111
175112
175113
175114
175115
175116
175117
175118
175119
175120
175121
175122
175123
175124
175125
175126
175127
175128
175129
175130
175131
175132
175133
175134
175135
175136
175137
175138
175139
175140
175141
175142
175143
175144
175145
175146
175147
175148
175149
175150
175151
175152
175153
175154
175155
175156
175157
175158
175159
175160
175161
175162
175163
175164
175165
175166
175167
175168
175169
175170
175171
175172
175173
175174
175175
175176
175177
175178
175179
175180
175181
175182
175183
175184
175185
175186
175187
175188
175189
175190
175191
175192
175193
175194
175195
175196
175197
175198
175199
175200
175201
175202
175203
175204
175205
175206
175207
175208
175209
175210
175211
175212
175213
175214
175215
175216
175217
175218
175219
175220
175221
175222
175223
175224
175225
175226
175227
175228
175229
175230
175231
175232
175233
175234
175235
175236
175237
175238
175239
175240
175241
175242
175243
175244
175245
175246
175247
175248
175249
175250
175251
175252
175253
175254
175255
175256
175257
175258
175259
175260
175261
175262
175263
175264
175265
175266
175267
175268
175269
175270
175271
175272
175273
175274
175275
175276
175277
175278
175279
175280
175281
175282
175283
175284
175285
175286
175287
175288
175289
175290
175291
175292
175293
175294
175295
175296
175297
175298
175299
175300
175301
175302
175303
175304
175305
175306
175307
175308
175309
175310
175311
175312
175313
175314
175315
175316
175317
175318
175319
175320
175321
175322
175323
175324
175325
175326
175327
175328
175329
175330
175331
175332
175333
175334
175335
175336
175337
175338
175339
175340
175341
175342
175343
175344
175345
175346
175347
175348
175349
175350
175351
175352
175353
175354
175355
175356
175357
175358
175359
175360
175361
175362
175363
175364
175365
175366
175367
175368
175369
175370
175371
175372
175373
175374
175375
175376
175377
175378
175379
175380
175381
175382
175383
175384
175385
175386
175387
175388
175389
175390
175391
175392
175393
175394
175395
175396
175397
175398
175399
175400
175401
175402
175403
175404
175405
175406
175407
175408
175409
175410
175411
175412
175413
175414
175415
175416
175417
175418
175419
175420
175421
175422
175423
175424
175425
175426
175427
175428
175429
175430
175431
175432
175433
175434
175435
175436
175437
175438
175439
175440
175441
175442
175443
175444
175445
175446
175447
175448
175449
175450
175451
175452
175453
175454
175455
175456
175457
175458
175459
175460
175461
175462
175463
175464
175465
175466
175467
175468
175469
175470
175471
175472
175473
175474
175475
175476
175477
175478
175479
175480
175481
175482
175483
175484
175485
175486
175487
175488
175489
175490
175491
175492
175493
175494
175495
175496
175497
175498
175499
175500
175501
175502
175503
175504
175505
175506
175507
175508
175509
175510
175511
175512
175513
175514
175515
175516
175517
175518
175519
175520
175521
175522
175523
175524
175525
175526
175527
175528
175529
175530
175531
175532
175533
175534
175535
175536
175537
175538
175539
175540
175541
175542
175543
175544
175545
175546
175547
175548
175549
175550
175551
175552
175553
175554
175555
175556
175557
175558
175559
175560
175561
175562
175563
175564
175565
175566
175567
175568
175569
175570
175571
175572
175573
175574
175575
175576
175577
175578
175579
175580
175581
175582
175583
175584
175585
175586
175587
175588
175589
175590
175591
175592
175593
175594
175595
175596
175597
175598
175599
175600
175601
175602
175603
175604
175605
175606
175607
175608
175609
175610
175611
175612
175613
175614
175615
175616
175617
175618
175619
175620
175621
175622
175623
175624
175625
175626
175627
175628
175629

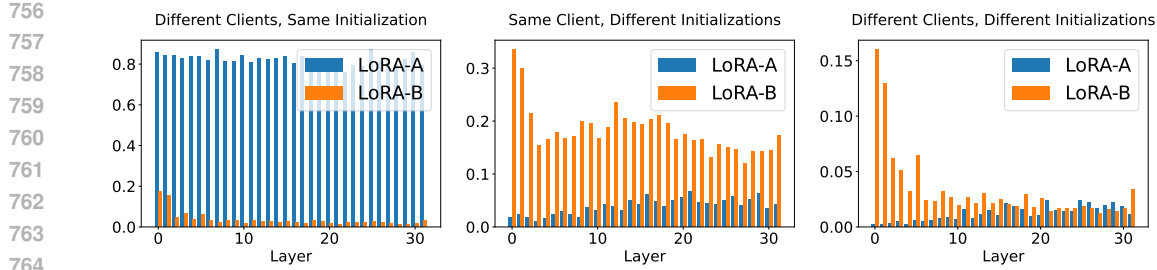


Figure 8: Layer-wise similarity analysis of LoRA modules across clients in federated fine-tuning. Left: two different clients with the same random seed. Middle: the same client with different random seeds. Right: two different clients with different random seeds. A_i matrices are similar only under the same initialization, whereas B_i exhibits relatively stable similarity across different clients and seeds.

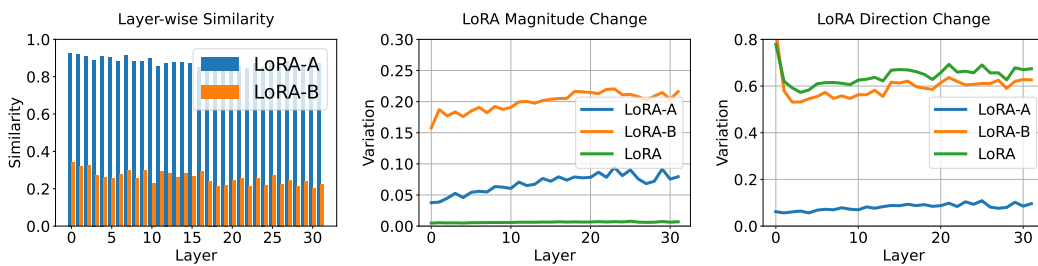


Figure 9: Comparison of LoRA modules on each client before and after federated fine-tuning. Left: similarity; Middle: magnitude change; Right: direction change. LoRA shows limited magnitude change, with nearly all directional change captured by B .

To further explore whether the above observation depends on the model or dataset, we analyze the learning dynamics of LoRA the Qwen2-7B (Yang et al., 2025)⁶ model using the bigscience/xP3 dataset (Muenninghoff et al., 2023), which contains data from 46 languages and 16 NLP tasks. We sample 3,000 English examples and fine-tune the model using the same configuration. The results are shown in Figure 10. We observe the same pattern: the B matrix plays a more dominant role than A matrix during training.

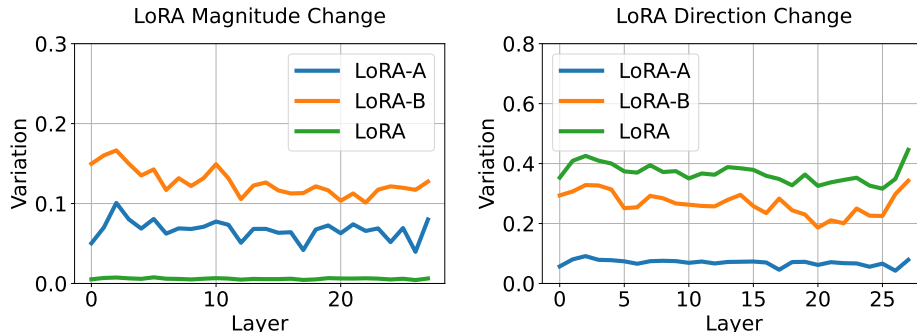


Figure 10: Comparison of LoRA modules using Qwen2-7B before and after federated fine-tuning. Left: magnitude change; Right: direction change.

A.3 PRACTICAL IMPLEMENTATION

For the results in Section 3.1–3.2, we fine-tune the LLaMA2-7B model on data sampled from the Dolly-15K dataset for 3 epochs. The training uses a learning rate of 3e-4, batch size 32, and gradient accumulation step 2. We follow the alpaca_short template (Taori et al., 2023) to construct the instruction data. LoRA is applied to the q_{proj} modules with rank $r = 8$.

⁶<https://huggingface.co/Qwen/Qwen2-7B>

810 For the analysis of lazy learning in multi-task fine-tuning (Section 3.3), we fine-tune the LLaMA3-
 811 8B model on the commonsense reasoning 15K dataset (Hu et al., 2023) for 3 epochs, using a learning
 812 rate of 3e-4, batch size 4, and gradient accumulation step 4. LoRA is applied to the q_{proj} modules
 813 with rank $r = 8$. The sharing- A structure uses 3 A matrices, and the sharing- B structure uses 3 B
 814 matrices.

815 For the analysis of knowledge transfer in federated fine-tuning (Section 3.3), we fine-tune the
 816 LLaMA2-7B model on the federated NLP dataset (Long et al., 2024) for 10 communication rounds,
 817 with 10 local epochs per client. The learning rate is 5e-4, the batch size is 32, and the gradient
 818 accumulation step is 2. In the homogeneous setting, all clients use rank 8. In the heterogeneous
 819 setting, the ranks are set to $\{64, 64, 32, 32, 16, 16, 8, 8\}$. The methods are applied to q_{proj} and v_{proj}
 820 modules. All experiments are conducted on RTX A6000 GPU.

821

822 B ADDITIONAL EXPERIMENTAL DETAILS AND RESULTS

823

824 B.1 BENCHMARKS

825

826 The intra-domain multi-task commonsense reasoning 170K benchmark contains questions from the
 827 following datasets: (1) ARC-Challenge and ARC-Easy (Clark et al., 2018), which consist of grade-
 828 school-level multiple-choice science questions; (2) BoolQ (Clark et al., 2019), a yes/no question-
 829 answering dataset requiring non-factoid reasoning and entailment; (3) HellaSwag (Zellers et al.,
 830 2019), a dataset of commonsense natural language inference (NLI) questions that require identi-
 831 fying the most appropriate continuation of a narrative input; (4) OpenBookQA (Mihaylov et al.,
 832 2018), which contains questions requiring multi-step reasoning by combining provided scientific
 833 facts with external background knowledge; (5) PIQA (Bisk et al., 2020), a dataset of everyday com-
 834 monsense reasoning questions about the physical world; (6) SIQA (Sap et al., 2019), which focuses
 835 on social and emotional commonsense reasoning in everyday human interactions; (7) WinoGrande
 836 (Sakaguchi et al., 2021), a collection of fill-in-the-blank sentences designed to test pronoun resolu-
 837 tion using commonsense.

838

839 The cross-domain multi-task NLP dataset contains 8 NLP tasks sampled from the FLAN dataset
 840 (Wei et al., 2022). The tasks are: (1) Commonsense, a reasoning task that requires everyday knowl-
 841 edge to make judgments; (2) Entailment, an NLI task that determines the relationship between a
 842 premise and a hypothesis; (3) Open-domain QA, a question answering task that retrieves or gen-
 843 erates answers from open sources; (4) Paraphrase, a classification task that recognizes whether a
 844 sentence pair is semantically equivalent; (5) Reading comprehension, a question answering task
 845 requires understanding the text content and answering the related questions; (6) Sentiment classifi-
 846 cation, a classification task that determines the whether the sentiment polarity is neutral, positive, or
 847 negative; (7) Summarization, an NLG task that produces a compact digest of a long passage while
 848 keeping the critical information; (8) Text formatting, an NLG task that corrects the punctuation in
 849 unformatted text. Each task has 300 examples for training and 200 examples for testing.

850

851 The federated NLP dataset also contains 8 NLP tasks sampled from the FLAN dataset (Wei et al.,
 852 2022). The tasks are: (1) Coreference, a discourse understanding task that requires determining
 853 which entity a pronoun refers to; (2) Entailment, an NLI task that determines the relationship be-
 854 tween a premise and a hypothesis; (3) Linguistic Acceptability, a classification task that detects
 855 whether a sentence is grammatical; (4) Paraphrase, a classification task that recognizes whether a
 856 sentence pair is semantically equivalent; (5) Question classification, a task for question under-
 857 standing in question answering systems; (6) Structure-to-Text, a natural language generation (NLG) task
 858 that converts structured triples into natural language; (7) Text formatting, an NLG task that corrects
 859 the punctuation in unformatted text; (8) Word sense disambiguation, a classification task that deter-
 860 mines whether the same word has the same meaning in two different sentences. Each task has 300
 861 examples for training and 200 examples for testing, and we assign one task to each client.

862

863 For the intra-domain multi-task fine-tuning, we also consider the math reasoning 10K benchmark
 864 (Hu et al., 2023), which includes 4 datasets: (1) AQuA (Ling et al., 2017), which contains multiple-
 865 choice algebra word problems, each accompanied by a natural language rationale explaining the
 866 step-by-step reasoning; (2) GSM8K (Cobbe et al., 2021), a high-quality collection of linguisti-
 867 cally diverse grade-school-level math word problems designed to evaluate multi-step reasoning; (3)
 868 MAWPS (Koncel-Kedziorski et al., 2016), a compilation of math word problems intended to support

robust and scalable research on arithmetic reasoning, including AddSub (basic addition/subtraction), SingleOp (single-operator arithmetic), MultiArith (multi-step arithmetic), SingleEq (single-equation algebra); (4) SVAMP (Patel et al., 2021), which consists of simple one-unknown grade-school-level arithmetic word problems, designed to test robustness in arithmetic reasoning.

The original split of the math reasoning 10K benchmark is not suitable for multi-task fine-tuning, since it does not include the full training data of the subsidiary tasks. In addition, Hu et al. (2023) report data leakage issues in this benchmark. To address these concerns, we downloaded the original data of each single task, and checked every training example in the benchmark to determine whether it belongs to the training set of any individual task. This process allowed us to construct a training dataset for each task, making it possible to fine-tune on single tasks and obtain single-task baselines. For multi-task fine-tuning, we fine-tune directly on the benchmark and evaluate on each task. Since the single-task training splits are created by us, we report the corresponding results in the Appendix.

B.2 BASELINES

For multi-task fine-tuning, we compare our ALoRA with the following methods: (1) the vanilla LoRA (Hu et al., 2022); (2) LoHa (Yeh et al., 2023), which employs Hadamard decompositions to the updates; (3) AdaLoRA (Zhang et al., 2023), which adaptively prunes rank using SVD; (4) MoSLoRA (Wu et al., 2024a), which introduces an additional matrix to fuse update subspaces; (5) HydraLoRA (Tian et al., 2024), which adopts a sharing- A multi-LoRA framework.

For homogeneous federated fine-tuning, we compare our Fed-ALoRA with the following methods: (1) FedIT (Zhang et al., 2024), where each client transmits the full LoRA parameters; (2) FedDPA (Long et al., 2024), which employs both a global adapter and a local adapter for each client; (3) FedSA-LoRA (Guo et al., 2025), which shares only the A matrices. For the heterogeneous federated fine-tuning, we compare Fed-ALoRA with: (1) ZeroPadding, which pads all heterogeneous ranks to the maximum rank across clients, enabling FedIT to support heterogeneity; (2) FLoRA (Wang et al., 2024), a stacking-based noise-free aggregation method; (3) FedSA-LoRA (Guo et al., 2025), which does not natively support heterogeneity but is adapted here using the decomposition proposed in our method.

B.3 PRACTICAL IMPLEMENTATION

For intra-domain multi-task fine-tuning on commonsense reasoning and math reasoning, we fine-tune the LLaMA3-8B model for 3 epochs on the training data with a learning rate of 3e-4. The AdamW optimizer is used with $\beta_1 = 0.9$ and $\beta_2 = 0.999$. The batch size is 4, and the gradient accumulation step is 4. For HydraLoRA, we follow the original setup with one single A matrix and 3 B matrices with rank 8. For our ALoRA, we use 3 A matrices and a single B matrix with rank 8. To ensure a fair comparison, the other baselines are configured with a comparable parameter size: LoRA, LoHa, and MoSLoRA use rank 16, while others use rank 8. All methods are applied to the q_{proj} and o_{proj} modules.

For cross-domain multi-task fine-tuning, we fine-tune the LLaMA2-7B model for 50 epochs on the training data with a learning rate of 3e-4. The AdamW optimizer is used with $\beta_1 = 0.9$ and $\beta_2 = 0.999$. The batch size is 4, and the gradient accumulation step is 4. For HydraLoRA, we follow the original setup with one single A matrix and 3 B matrices with rank 8. For our ALoRA, we use 3 A matrices and a single B matrix with rank 8. To ensure a fair comparison, the other baselines are configured with a comparable parameter size: LoRA, LoHa, and MoSLoRA use rank 16, while others use rank 8. All methods are applied to the q_{proj} and v_{proj} modules.

For federated fine-tuning, we fine-tune the LLaMA2-7B model for 10 communication rounds with 10 local epochs per client, using a learning rate of 5e-4. The AdamW optimizer is used with $\beta_1 = 0.9$ and $\beta_2 = 0.999$. The batch size is 32, and the gradient accumulation step is 2. In the homogeneous setting, all clients use rank 8. In the heterogeneous setting, the ranks are set to $\{64, 64, 32, 32, 16, 16, 8, 8\}$, and d_m is chosen to 16. All methods are applied to q_{proj} and v_{proj} modules. All experiments are conducted on RTX A6000 GPU.

918
919 Table 7: Results on math reasoning. $\Delta m\%$ measures performance balance across tasks. ALoRA
920 achieves the most balanced results.
921

Method	AQuA	GSM8K	SVAMP	MAWPS	SingleEq	Avg.	$\Delta m\%(\downarrow)$
Single	28.34	63.68	71.10	86.13	90.75	68.00	
LoRA	30.31	66.26	75.10	90.34	94.88	71.38	-5.21
LoHa	27.56	63.84	76.70	90.76	94.88	70.75	-3.06
AdaLoRA	25.20	59.44	72.60	86.55	91.93	67.14	2.77
MoSLoRA	28.74	67.40	77.10	89.08	94.06	71.28	-4.54
HydraLoRA	27.17	68.76	75.60	90.34	93.31	71.04	-3.58
ALoRA	29.53	67.17	77.40	89.50	94.49	71.62	-5.31

930
931 Table 8: Results of different intermediate ranks in the heterogeneous setting.
932

Fed-ALoRA	Coref	Ent	LAcc	Para	QCls	S2T	TFmt	WSD	Avg.	$\Delta m\%(\downarrow)$
$d_m = 8$	90.75	84.50	79.50	73.50	95.00	73.05	96.09	63.00	81.92	-0.41
$d_m = 16$	88.27	89.50	79.50	77.00	94.00	72.35	96.37	63.00	82.50	-1.07
$d_m = 32$	88.63	86.50	78.00	79.00	94.00	72.27	96.60	63.00	82.25	-0.80
$d_m = 64$	85.70	89.00	81.00	75.50	94.00	72.31	96.40	65.00	82.37	-1.01

937 938 B.4 ADDITIONAL EXPERIMENT RESULTS

939
940 The results on the math reasoning benchmark are presented in Table 7. LoRA, MoSLoRA, and our
941
942 ALoRA outperform the single-task baseline on all tasks, but ALoRA achieves the most balanced
943
944 performance, showing that it enables more effective knowledge transfer than the baselines. We also
945 provide the full results of the study of different intermediate ranks in Section 5.3, which are shown
946 in Table 8.

947
948 To further compare the effectiveness of sharing A and sharing B , we provide an additional study
949
950 of HydraLoRA and our ALoRA using Qwen2-7B (Yang et al., 2025)⁷ and LLaMA2-13B (Touvron
951
952 et al., 2023)⁸. We fine-tune the models using the same configuration as before, and report the mean
953
954 and standard error over 3 independent runs for Qwen-7B. The results on LLaMA2-13B are less
955
956 stable, likely because the configuration is suboptimal for the larger model, so we report only the best
957
958 result from 3 runs. The comparisons shown in Table 9 validate that ALoRA consistently outperforms
959
960 HydraLoRA.

961
962 Table 9: Comparison between HydraLoRA and ALoRA on intra-domain multi-task commonsense
963
964 reasoning benchmark.

Method	ARC-C	ARC-E	BoolQ	HellaS.	OBQA	PIQA	SIQA	WinoG.	Avg.
HydraLoRA (Qwen-7B)	84.60 ± 0.30	93.20 ± 0.03	73.37 ± 1.42	94.42 ± 0.36	88.30 ± 0.42	89.58 ± 0.72	80.97 ± 0.06	84.33 ± 0.95	86.09 ± 0.42
ALoRA (Qwen-7B)	85.28 ± 0.42	93.69 ± 0.30	73.41 ± 0.15	94.76 ± 0.36	90.10 ± 0.42	89.07 ± 0.07	80.94 ± 0.47	84.50 ± 0.50	86.47 ± 0.07
HydraLoRA (LLaMA2-13B)	59.90	66.46	72.42	56.46	66.80	83.95	74.26	83.50	70.47
ALoRA (LLaMA2-13B)	74.40	86.03	74.43	67.62	82.80	79.87	80.71	76.96	77.86

965 966 C THE USE OF LARGE LANGUAGE MODELS (LLMs)

967
968 In preparing this manuscript, large language models (LLMs) were used only to assist with language
969
970 polishing and stylistic refinement. All technical content, formulations, experimental designs, and
971
972 conceptual contributions were developed by the authors. Importantly, LLMs were not used for
973
974 ideation and methodology development.

7⁷<https://huggingface.co/Qwen/Qwen2-7B>

8⁸<https://huggingface.co/meta-llama/Llama-2-13b-hf>